Proceedings of the ASME 2019 38th International Conference on Ocean, Offshore and Arctic Engineering
OMAE2019
June 9-14, 2019, Glasgow, Scotland,UK

OMAE2019-96079

NUMERICAL STUDY OF A SINGLE-POINT MOORING GRAVITY FISH CAGE WITH DIFFERENT DEFORMATION-SUPPRESSION METHODS

Hui Cheng
Department of Mechanical and Structural
Engineering and Materials Science,
University of Stavanger
4036, Stavanger, Norway
Email: hui.cheng@uis.no

Karl Gunnar Aarsæther
SINTEF Ocean
7465 Trondheim, Norway
Email: karl.gunnar.aarsather@sintef.no

Lin Li
Department of Mechanical and Structural
Engineering and Materials Science,
University of Stavanger
4036, Stavanger, Norway
Email:lin.li@uis.no

Muk Chen Ong
Department of Mechanical and Structural
Engineering and Materials Science,
University of Stavanger
4036, Stavanger, Norway
Email: muk.c.ong@uis.no

ABSTRACT

Compared to the multi-point mooring fish cage, the single point mooring (SPM) fish cage can spread out the accumulation of organic matter to prevent the local environment from being overwhelmed, and reduce the manufacturing cost at the same time. Thus, it has attracted many attentions recently. In this research, different deformation-suppression methods are applied to the SPM system with a typical Norwegian fish cage aiming to reduce the cultivation volume loss. A well-validated software, FhSim, is used to conduct the full-scale numerical study. The effects of the three deformation-suppression methods (i.e. (i) adding the lower bridles, (ii) adding the frontal rigid frame, (iii) adding the trawl door) are analyzed under pure current and combined wave-current conditions. The results indicate that all the three methods can reduce the cultivation volume loss at least by 32% compared to the one with the original SPM system when the current velocity is larger than 0.5 m/s. In addition, moving the conjunction point close to the bottom ring can bring positive effect in the cultivation volume maintaining with an unnoticeable increase in the tension force. This study will provide practical advice and useful guides for the SPM fish cage design.

INTRODUCTION

Aquaculture has been the world's fastest growing food production sector in the past 40 years. With over one-third of aquaculture produced in marine waters and this proportion increasing, concerns about pollution and health have increased markedly [1]. The deteriorated marine environment around the fish farm has been criticized by environmentalists because the potential waste pollution, such as uneaten feed and fish wastes, accumulates on the seabed and causes water contamination [2]. The impact depends on the fish cage design, culture operation and the local environment in which it is located. To reduce environmental stress, an alternative approach is to allow cages to move in response to the environment. For instance, the use of a single point mooring (SPM) would allow the aquaculture system to maintain a watch circle where the position of the cage depends on the sum of the environmental forces [1].

The concept of SPM fish cage was proposed in recent years and received many attentions for its eco-environment benefit. Compared to the conventional multi-point mooring fish cage, the single-point mooring fish cage can rotate around the anchor point according to the changing wave and current directions. This enables the system to accommodate waves and current rather than resist them. Moreover, fish wastes and unconsumed feed can be dispersed in a large area, and thus considerably minimize the impact on the seabed. Preliminary research of the benefits of SPM indicates a two to 70 times reduction in deposition of waste on the seabed, depending on current and mooring design [1]. Furthermore, because of the simplification of the mooring system, SPM fish cage could reduce the cost up to 50% compared to the conventional multi-point mooring fish cage [3]. The mooring cost can be reduced more when the fish cages are grouped together and moved to exposed water. In addition, adopting the SPM system may reduce the gap period for the cage culture, which will improve the profit for aquaculture companies.

There are two important issues in fish farm design: the maximum tension force of the mooring system and the volume reduction of the fish cage subjected to current and waves. The tension forces on the anchor line and bridles will increase when using the SPM system because all the forces will be summed to the only existed anchor line. However, it has been noted that the maximum total loading on the array moored fish cage can be reduced especially when the anchor extends in the direction of the array's major axis [1]. For the other cage deformation, several attempts have been made to improve the fish cage deformation and minimize the volume reduction. According to previous researches [4, 5], increasing the sinker weight can improve the cultivation volume to a certain degree. Huang et al. [6] used a numerical method to investigate the effect of an SPM fish cage system with a rigid frontal frame. The rigid frame improves the volume reduction coefficient from 64% to 31% in harsh conditions according to their results. In Xu et al's research [7, 8], they have compared two different mooring systems to improve self-submersible SPM fish cage deformation: one adopts lower bridles, the other adopts a rigid frame which is similar to Huang et al's research [6]. In addition, there are some engineering cases adopting the lower bridles to control the deformation [9–11]. However, a systematic understanding of how the lower bridles contribute to deformation suppression is still lacking.

Up to now, there has been no research combining the single-point mooring system to a large fish cage. Previous studies of deformation-suppression methods have only carried out on a small scale (less than 10 meters deep and 20 meters in diameter). Now in Norway, a typical net cage is 20-50 meters in depth and 50 meters in diameter [12]. According to the previous method [7], larger fish cage requires a larger front frame to keep its shape. However, a large front frame might become less stable and easier to bend in the harsh environmental conditions. This indicates a need to assess the feasibility of the previous deformation-suppression methods in a large fish cage.

In this study, three different deformation-suppression methods are applied to a typical Norwegian fish cage to study their mooring force and fish cage volume under the action of currents and/or waves. The first two methods ((i) adding the lower bridles and (ii) adding the rigid frame) are based on the previous studies [6, 7]. Moreover, a new method is proposed, using the trawl door concept from fishing science, to reduce the deformation of the SPM fish cage. This new object will be tested and evaluated jointed with the previous two methods. Firstly, the description of the Norwegian fish cage with different mooring system is given. Then, the effects of different deformation-suppression methods on the cage structure are studied and compared under pure current conditions. Next, their performances under combined wave-current conditions are studied. Finally, conclusions and suggestions are given.

DESCRIPTION OF THE SPM FISH CAGE SYSTEM

A typical Norwegian fish cage is chosen for the present study. The fish cage includes a double-pipe floating collar, a cage net (cylindrical net structure with conical bottom), cables (connecting cage net and sinker tube), a sinker tube and a centre point weight. A basic SPM system would include an anchor line, a buoy line, a conjunction point, a buoy and some bridles. The parameters of the Norwegian fish cage are listed in Table 1, and the schematic description of the fish cage with the SPM system is shown in Figure 1.

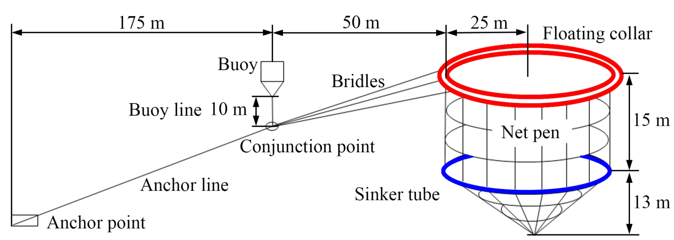

FIGURE 1. Schematic description of a typical Norwegian fish cage with SPM system.

A schematic description of the three different deformation-suppression mooring systems is shown in Figure 2. More detailed descriptions of the mooring system are listed as follows:

(a) In the first method, only three lower bridles are added, based on its counterpart, to connect the conjunction point and sinker tube (see Figure 2(a)). This method is the simplest and cheapest compared to the following two methods.
(b) In the second method, a frontal rigid frame is placed between the fish cage and conjunction point. It is made of high-density polyethylene (HDPE) tube and can be decomposed into three segments: the top segment that is hollow

TABLE 1. Specifications of a typical Norwegian fish cage.

Component	Dimension name	Value	Unit
Floating collar	Inner pipe diameter	50.97	m
	Outer pipe diameter	52.97	m
	Pipe section diameter	0.25	m
	Pipe thickness	28.4	mm
	Pipe bending stiffness	9E8	Nm^2
Cage net	Cage height	15	m
	Bottom cone depth	13	m
	Net twine density	1125	kg/m^3
	Net twine E-modulus	1E8	Nm^2
	Net twine diameter	2.5	mm
	Net mesh length	25	mm
	Solidity ratio	0.2	-
Cables	Cables length	2.5	m
	Cable diameter	0.35	m
	E-modulus	1E9	Nm^2
Sinker tube	Tube diameter	50	m
	Section diameter	0.25	m
	Initial depth	17.5	m
	Tube weight	51	kg
	Centre point weight	981	kg

and floating at the water surface; the side segment that is filled with water and submerged in the water; and the bottom segment that not only is inserted with an iron chain but also with water to keep the frame vertically floating in the water. The frame is 19.5m in width and 17.5m in height in this study (see Figure 2(b)). More information about the frontal rigid frame can be found in [3, 7].

(c) In the third method, trawl doors are adapted to replace the frontal rigid frame. The trawl doors are attached to the lower and upper rigid segment on each evenly distributed three foils, and the side segments are removed simultaneously (see Figure 2(c)). The upper foil will provide upward force and the lower foil will provide downward force. The trawl door can be made of iron and wood to adjust its centre of gravity and buoyancy. Its geometrical shape is a rectangular cambered structure, and its main dimensions are equivalent to a span of l= 2.2 m and a chord of c=2.0 m. The lift and drag coefficients in the working condition are 1.919 and 0.577, respectively. More geometrical and hydrodynamic data can be found in [13].

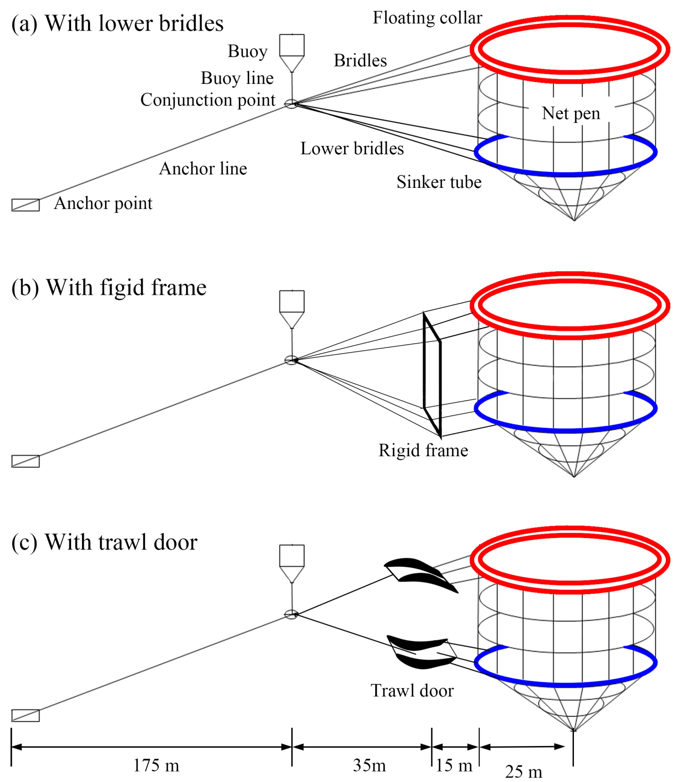

FIGURE 2. Schematic diagram of the typical Norwegian fish cage with different SPM systems: (a) with lower bridles (LB); (b) with rigid frame (RF); (c) with trawl doors (TD).

NUMERICAL METHODS
The FhSim Framework

FhSim is a time-domain simulation tool that has been under constant development at SINTEF Ocean (previously named SINTEF Fisheries and Aquaculture) since 2006, and has served as the primary platform for software development through a series of research projects [14]. Model development in FhSim is modular, in that models of complex systems are created by modelling the sub-components in the system as separate sub-models and then interconnecting these using input/output ports facilitating the necessary exchange of information [15].

At present, FhSim contains mathematical models relevant for simulating aquaculture structures, such as floating collars, generic net structures, cables/chains/ropes, buoys and sinker tubes. All the model has previously been validated through comparison with experimental data, showing satisfactory results, par-

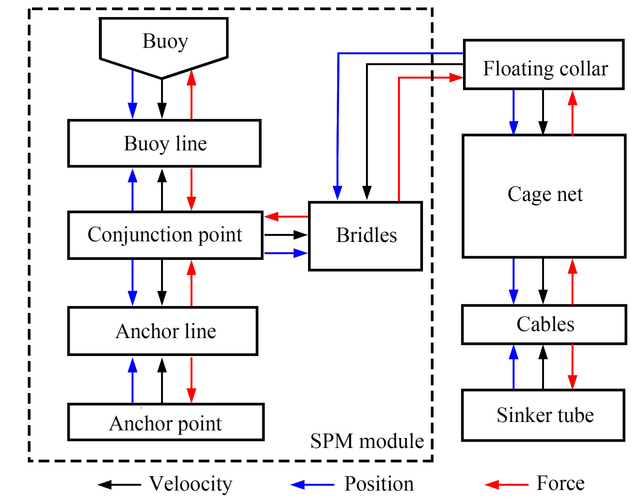

FIGURE 3. Flow chart of how variables are transferred and objects are connected in the simulation.

ticularly for low current velocities where the deviations are as low as 7% [15, 16].

In the present study, the FhSim framework is used for a comparative study regarding the three different deformation-suppression methods. Figure 3 shows a general description of how variables are transferred and objects are connected in the SPM fish system (shown in Figure 1). To improve the computational efficiency, a newly compiled SPM system module (see the dashed box in Figure 3) is implemented to the previous model [15] to replace its multi-point mooring system. The floating collar, cage net, cables and sinker tube are consistent with the previous model. Due to all the objects in the mooring system are packed into one module, the SPM module, the initial setup becomes easy and the variables exchange becomes efficient. Thus the computational time is highly reduced.

Hydrodynamic model

In this model, the SPM cage system is assumed to be deployed in the environment with uniform water depth. The fish cage system would be subjected to environmental loads, such as wave forces, current forces and wind forces. The wind forces on the floating collar are neglected in dynamic computation because only a small part of the floating collar is exposed to the air. Undisturbed water flow is assumed and wave particle velocity is superimposed in addition to the current. Hydrodynamic loads acting on the net elements are computed as the sum of the forces acting on the individual mesh bars and knots comprising the element, with each mesh bar being regarded as a smooth cylinder while each knot is considered a sphere. The computation of the drag forces acting on the mesh bars are divided into two separate equations handling the drag forces acting normally (F_N) and tangentially (F_T) on the mesh bars (Figure 4, Eqn. 1, Eqn. 2). It can be referred to [17] for more information on the hydrodynamic model.

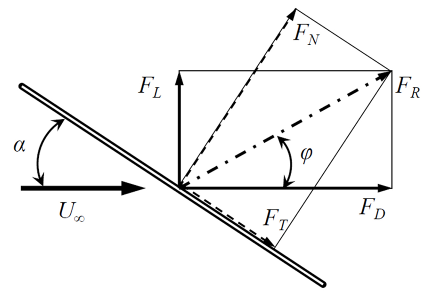

FIGURE 4. Hydrodynamic forces on a net panel: Drag (F_D), Lift (F_L), Normal force (F_N),Tangential force (F_T) and Resultant force (F_R).

$$F_N = \frac{1}{2}\rho A C_N |U_N| U_N \tag{1}$$

$$F_T = \frac{1}{2}\rho A C_T |U_T| U_T \tag{2}$$

The expressions U_N and U_T represent the normal and tangential component of relative velocity ($U_\infty - V_{net}$), where V_{net} is the velocity of the net and U_∞ is the incoming velocity. The terms C_N and C_T are the normal and tangential drag coefficients. Whereas C_T is assigned an approximate value of 0.01, the value of C_N comes from experimental data [18], and is defined as a seventh order polynomial function of the logarithmic Reynolds number (($\log_{10} Rn$) for the Reynolds number range $32 \leq Re \leq 10^4$ (Eqn. 3).

$$\begin{aligned} C_N = &-78.46675 + 254.73873(\log_{10} Rn - 327.8864(\log_{10} Rn)^2 \\ &+223.64577(\log_{10} Rn)^3 - 87.92234(\log_{10} Rn)^4 \\ &+20.00769(\log_{10} Rn)^5 - 2.44894(\log_{10} Rn)^6 \\ &+0.12479(\log_{10} Rn)^7 \end{aligned} \tag{3}$$

where $Rn = \frac{U_{net} d_t}{\nu}$ and $U_{net} = \frac{\sqrt{2-Sn}}{\sqrt{2}(1-Sn)} U_\infty$. d_t is the twine diameter; ν is the kinematic viscosity of water; S_n is solidity ratio.

The wake inside the cage net due to current plays an important role in numerical simulation. In this study, a model for turbulent wake is used to estimate the reduction in velocity behind twines in the cage net. Both element-internal (local) wake effects and inter-elemental (global) wake effects are calculated based on Blevins virtual origin formula [19]. The normalized velocity deficit downstream from a 2D circular cylinder placed at the origin (x=0, y=0) is given as:

$$\frac{U}{U_\infty} = 1.2\sqrt{\frac{C_d}{6+x/d}}\exp\left\{\frac{-(y/d)^2}{0.0767C_d(6+x/d)}\right\} \tag{4}$$

where U is the velocity reduction experienced at the coordinate. The positive x-axis is oriented along the incident velocity vector, C_d is the Reynolds number dependent drag coefficient for a circular cylinder and d is the cylinder diameter. It can be referred to [16] for more information on the wake effect.

Structural model

Cables, ropes and other components with cable-like properties are modelled using bar elements. The floating collar is modelled as a flexible continuous circular ring with 6 Degrees Of Freedom (DOF) with regards to rigid body motion. The sinker tube is modelled using a version of the generic cable model in which the two endpoints are connected to create a continuous cable structure. The buoy is modelled as vertical circular cylinders with a conical bottom. It is given 5 DOF where rotation around its vertical axis is omitted [20].

The net structure is calculated based on a well-established method, in which net panels of arbitrary shape are described by dividing the original shape into triangular net elements [21]. Structural forces acting within the structure are computed separately for each net panel and then distributed between the nodes associated with the panel element. It can be referred to [15, 17] for more details on the net structure model in FhSim.

FhSim supports the use of several different integration methods, including Euler methods, Heuns method and Runge-Kutta methods, and facilitates a suitable framework for implementing additional methods [14]. In this study, it employs a Runge-Kutta 45 method with variable time steps to solve the motion equation.

Volume calculation method

To compute the fish cage deformation, it is appropriate to consider the net pen as a stack of pies as shown in Figure 5. There are total m layers of pie, and each pie has n vertexes around it. We may choose an arbitrary point (o) as origin and define n vectors $\vec{op}_j$. Using the principle of vector cross product, we can compute the area of each layer (S_i) according to Eqn. 5, where P_{n+1}=P_1. In practical, the origin of global coordinate (0,0,0) is chosen as the starting point for all the n vectors, because the starting point can be either inside or outside the area.

$$S_i = \sum_{j=1}^{n} S_{\Delta OP_jP_{j+1}} = \frac{1}{2}|\sum_{j=1}^{n}(x_j y_{j+1} - x_{j+1} y_j)| \tag{5}$$

$$Volume = \sum_{i=1}^{m}\frac{1}{3}\Delta h_i(S_i + S_{i+1} + \sqrt{(S_i S_{i+1}}) \tag{6}$$

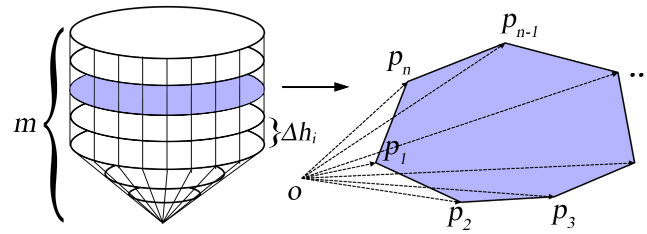

FIGURE 5. Fish cage volume divisions and its computing scheme.

TABLE 2. Parameters of waves and currents.

Case	Current V (m/s)	Wave height H (m)	Wave length L (m)
C0.25	0.25	0	0
C0.5	0.5	0	0
C1.0	1.0	0	0
C0.25H2L50	0.25	2	50
C0.25H2L75	0.25	2	75
C0.25H2L100	0.25	2	100
C0.5H2L50	0.5	2	50
C0.5H2L75	0.5	2	75
C0.5H2L100	0.5	2	100

The volume of each pie is calculated based on frustum of a skewed prism, where Δh_i is the height of each prism. Summing up the volume of all the pies, an approximate volume of the fish cage is obtained (Eqn. 6). Its accuracy depends on the number of nodes in the numerical model. In this study, a fish cage volume remaining coefficient is applied to represent the deformation of the net cage:

$$C_v = V_t/V_0 \tag{7}$$

where V_0 is the initial fish cage volume in still water, V_t is the transient volume of the fish cage exposed to waves and/or current.

RESULTS AND DISCUSSION
Environmental loading

In this study, three typical current velocities (low: 0.25 m/s, moderate: 0.5 m/s, high: 1.0 m/s) are chosen in the environmental setting (Table 2). For the pure current condition, the current is assumed to be steady and uniform over the entire water depth.

For the combined wave-current condition, the waves and current are adopted with the same direction in this study. Linear waves are applied based on the Airy wave theory. The wavelengths are set as 50, 75 and 100 m, which equal to 1, 1.5 and 2 times of the diameter of the fish cage. The effect of mooring systems on the deformation of the cage net and the tension force on the anchor point are investigated under the conditions in Table 2. Their performances are compared after the simulations reach the equilibrium.

Cage deformation and mooring force under current conditions

Adopting deformation-suppression methods can reduce the volume reduction. Figure 6 shows the fish cage volume-remaining coefficients with four different mooring systems under current conditions after equilibrium. All the fish cage volume whether with or without the deformation-suppression methods are decreased with the increasing velocity. However, the cages with deformation-suppression methods can have less volume reduction compared to the original fish cage especially when the current velocity is higher than 0.5 m/s. When the current velocity is low, the discrepancy among the three methods is very small; when the current velocity is high, the discrepancy appears obviously. The trawl door has the best performance in the high current velocity. However, it falls behind to the frontal rigid frame in the moderate current. Although the method using lower bridles is not the best, it can still increase the fish cage volume coefficient at least by 30% compared to its counterpart when the current velocity is higher than 0.5 m/s. This conflicting with Xu et al's results [7] could be possibly due to the discrepancy on the buoyancy of the buoy and the position of conjunction point. More explanations can be found in the following section.

Figure 7 shows the final steady state of the fish cage with four types of mooring systems when the current velocity = 1.0 m/s. It indicates that the original fish cage (without any deformation-suppression method) loses a huge cultivation volume in the harsh environment. The figure also shows the trawl door can significantly increase the height between the connecting points on the floating collar and sinker tube under the high current condition. Therefore, the deformation of the fish cage is suppressed significantly. The vertical distance between the upper and lower trawl door can maximally reach to 27 m, which is almost 1.5 times the height of the frontal rigid frame. In addition, the frontal frame has a pitch movement under the high current condition. This movement can reduce its separating effect. There is one thing we should notice when we analyze the deformation and displacement: the floating collar is located on the sea level even though the current velocity is very high. Thus, the available cultivation volume is mainly dependent on the depth of the sinker tube. Holding the sinker tube in a deeper position can improve the cultivation volume significantly.

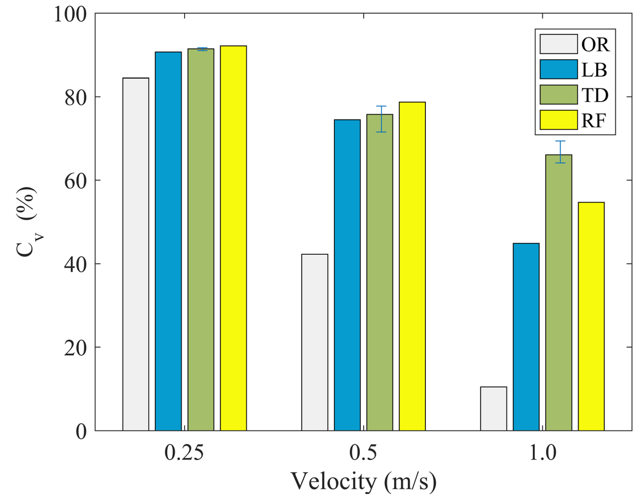

FIGURE 6. Fish cage volume remaining coefficient under different current velocities. (OR: the original SPM fish cage, LB: adding lower bridles, TD: adding trawl doors, RF: adding a front rigid frame.)

The tension force on the anchor point increases with the increasing current velocity. From the results in Figure 8, the tension force of the case with trawl door is the largest compared to the other methods under the same current velocity. That is not only because the larger projection area of the net pen can cause more drag force, but also the trawl door can bring extra drag force, which all the drag forces contribute to the increase of the tension force on the anchor point. The mean tension force with trawl door is almost 1.5 times of the original SPM fish cage when the current velocity is 1.0 m/s. The discrepancies of the tension force between the original SPM fish cage and lower bridles are less than 10%, which means the drag forces on the lower bridles have a negligible contribution to the tension force on the anchor point.

In addition, there are dynamic fluctuations in the volume and tension force for the case with the trawl door (Figure 6 and Figure 8). The error bars in the results represents the dynamic range of volume remaining coefficient or tension force. This phenomenon is caused by the motion of the upper foil, which floats up and down around the free surface, because the upper foil is very close to the free surface in this study. The upper foil can move out from the free surface due to the increased lift force. Then, the lift force becomes small and it causes the upper foil falls back into the free surface. This looping motion of the upper foil causes the unstable response. However, this should and could be avoided through further design optimization.

Cage deformation and mooring force under combined waves and current conditions

The waves increase environmental loads on the fish cage system. To analyze how the waves affect the cultivation volume

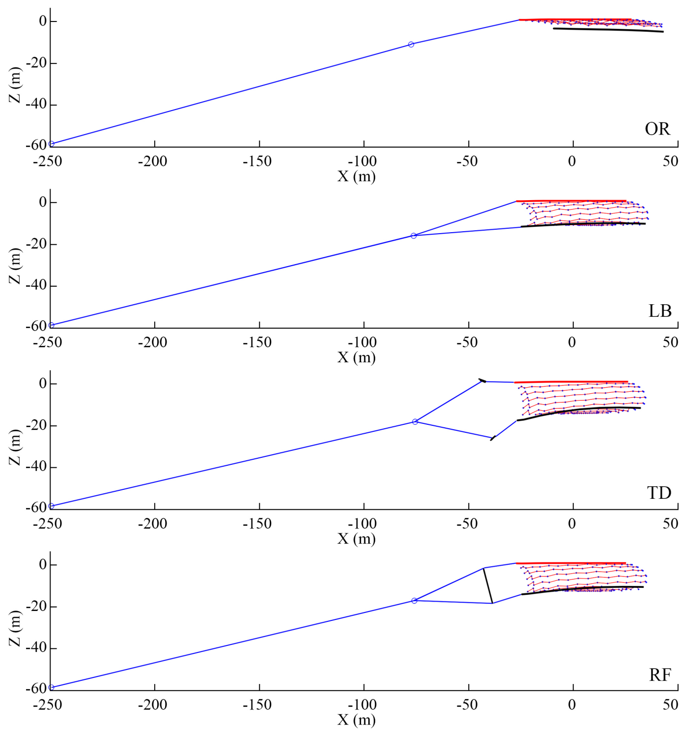

FIGURE 7. Deformation of the SPM fish cage in the final steady state when current velocity =1.0 m/s.

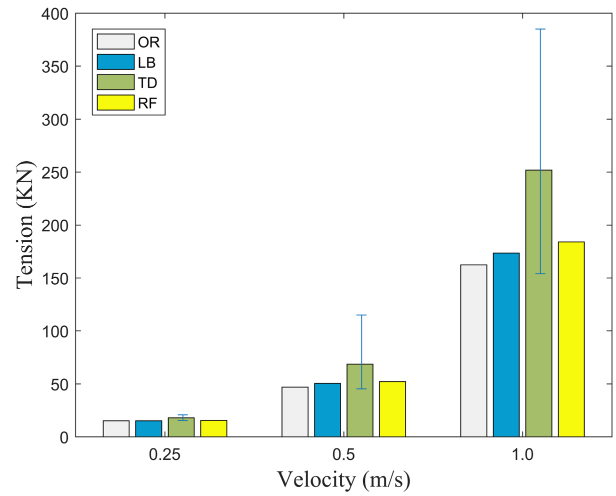

FIGURE 8. Tension forces on the anchor point under different current velocities. (OR: the original SPM fish cage, LB: adding lower bridles, TD: adding trawl doors, RF: adding a front rigid frame.)

and tension force, the time history of the response for the OR and LB in different environmental conditions is given in Figure 9. In this study, a pure current condition (v=0.5m/s) is applied in the simulation during the first 600s. Then waves are added into the continuous simulation until the end of the simulations. The wavelengths are 50, 75 and 100m with a constant wave height 2m (Table 2).

Figure 9(a) shows the volume remaining coefficient of the two cases under different environmental conditions. It indicates that whenever under current or combined wave-current conditions, the cultivation volume with the original mooring system is always smaller than the one with lower bridles. Under the pure current condition, lower bridles can increase 30% cultivation volume compared to the original SPM fish cage. Adding the waves can reduce the mean cultivation volume and bring periodic fluctuation on the cultivation volume. The amplitude and the mean value of cultivation volume are both increased with the wavelength. According to the Airy wave theory, the maximum wave particle velocity is decreased with the increasing wavelength. The maximum wave particle velocity at the free surface is approximately equal to 1.1 m/s when the wavelength is equal to the fish cage diameter. This means the wave particle velocity rises doubled at the free surface compared to the current velocity. Thus, it can bring a significant wave load on body net near the free surface, and the cultivation volume will shrink a lot. The snapshots in Figure 9(a) indicate that the body net of the original fish cage is very close to the free surface where the high hydrodynamic load will lead to large deformation, and thus the cultivation volume shrinks significantly. However, the lower bridles can hold the sinker tube and control its upwards motion, so the cultivation volume reduces only in a small degree. To explain why the dynamic amplitude of the cultivation volume is increased with the increasing wavelength, the motion properties of the floating collar and sinker tube need to be analyzed under combined wave and current condition. Because the motions of the floating collar and sinker tube are highly affected by the water particle velocity which is decreased with the increasing water depth, the sinker tube is relatively stable compared to the floating collar. Thus, the dynamic change of cultivation volume mainly comes from the motion of the floating collar. When the wavelength is smaller than the diameter of the fish cage, the effect of wave loads on the fish cage is small. Thus, the amplitude of the dynamic cultivation volume is reduced with the decreasing wavelength.

Figure 9(b) shows the results of the tension force on the anchor point under pure current and combined wave-current conditions. In the first 600 s, the tension force with the original mooring system is 7% smaller than the one with lower bridles. However, the tension force increases significantly when the waves exist. For the original fish cage without the lower bridles, the body net floats upwards when the water velocity is high. At the same time, the upward movement into the wave zone brings additional loads from high water particle velocity to drive it more upwards. Consequently, the tension force on the anchor point will increase compared to the case under pure current condition. Because the

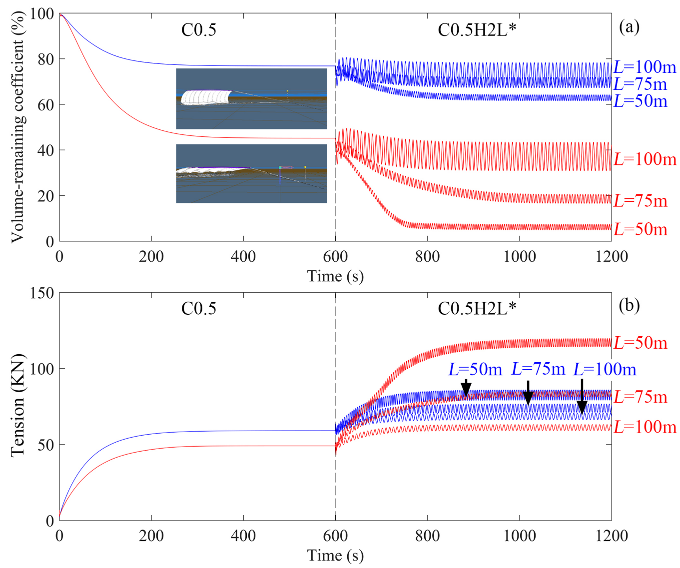

FIGURE 9. Wave effect on (a) the fish cage volume remaining coefficient and (b) the tension force on the anchor point (red: the original SPM fish cage; blue: adding lower bridles).

body net floats to the free surface where the maximum wave particle velocity is almost twice the current velocity, the total drag force on the net will increase rapidly. Under the combined wave and current conditions, the tension force increases with fluctuation: the mean value of the tension force is increased with the decreasing wavelength; the amplitude of the tension force almost keeps in the same. According to Zhao et al's study [22], the wave drift forces acting on the porous media is decreased with the increasing wavelength in a certain range. Therefore the mean value of the tension force is decreased with the increasing wavelength in this study. These numerical results have the same trend as the previous experimental study [23].

The fish cage volume-remaining coefficients of the fish cage with four kinds of mooring system are shown in Figure 10. In this figure, the mean value of the volume-remaining coefficient is represented by the bar height, and the dynamic range is represented by the error bars. The results show that the mean value and the amplitudes of the cultivation volume are increased with the increasing wavelength. The trawl door and the frontal rigid frame have almost the same effect in the cultivation volume improvement under the combined wave-current condition. Although the lower bridles are not as efficient as the trawl door and the frontal frame in the volume maintaining, it still increases the mean value of cultivation volume as low as by 3% in comparison with the original mooring system. For the mean cultivation volume of the original SPM fish cage, it shrinks more than 60% when the wavelength is less than 75 m compared to it under the pure condition.

Results of the tension force on the anchor point with different mooring systems are shown in Figure 11, where the bar height represents the mean tension force and the error bars represent the dynamic range. As shown in Figure 11, the amplitude and the mean value of tension force are decreased with the increasing wavelength. According to the Airy wave theory, increasing the wavelength will lead to a decrease in the amplitude of the wave particle velocity. This will lead to a reduction in the amplitude of hydrodynamic forces on the net because the forces are proportional to the second order of water velocity (Eqn. 1, Eqn. 2). In addition, the wave steepness is decreased with the in-

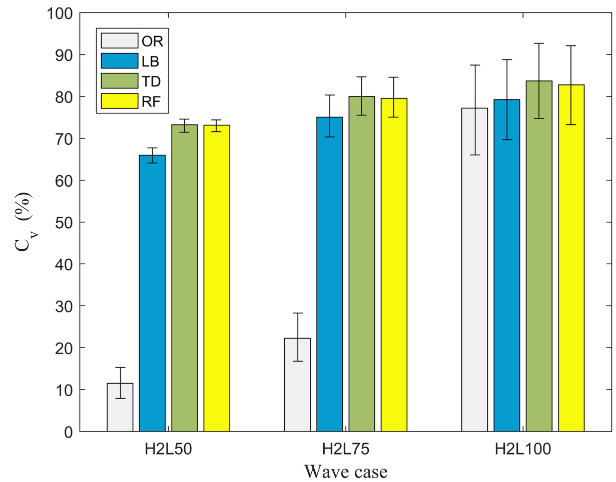

FIGURE 10. Fish cage volume remaining coefficient under combined waves and current, where the current velocity=0.25m/s. (OR: the original SPM fish cage, LB: adding lower bridles, TD: adding trawl doors, RF: adding a front rigid frame.)

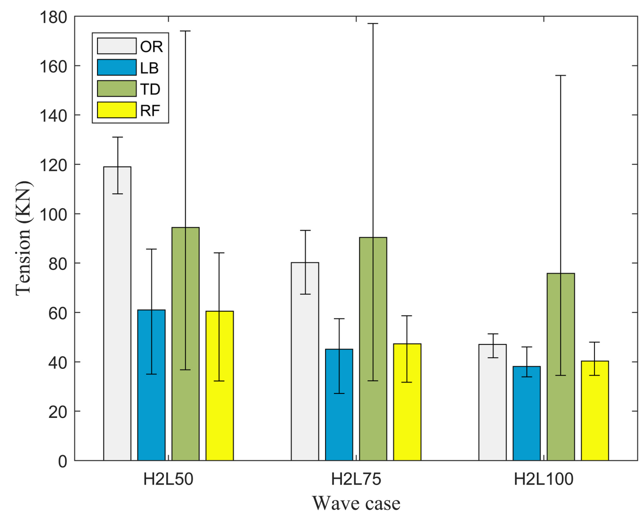

FIGURE 11. Tension force on the anchor point under combined waves and current, where the current velocity=0.25m/s.

creasing wavelength due to the constant wave height. According to the experimental study [23], the tension force on the anchor point is reduced with the increasing wave steepness. The tension force with trawl door is the largest because the trawl door can impose extra drag force on the mooring system and increase the tension force on the anchor point. Moreover, the upper foil is located in the near free surface layer, where the high wave particle velocity can induce large dynamic forces. The mean tension forces with lower bridles and the rigid frame are very similar, and surprisingly both of them are smaller than the one with the original mooring system. This indicates that holding the bottom ring in a deep position can reduce the total drag force on the body net. Another reason for the high mooring force with the original mooring system may be the model deficiency: e.g. the disordered net (which is close to the free surface) does not give an appropriate shadowing effect. Mooring system resonance due to harmonic wave excitation can be experienced in flexible aquaculture moorings. However, the present study only includes a limited set of wave periods. More dynamic analyses with a larger set of wave periods are needed in order to analyze possible resonance effects.

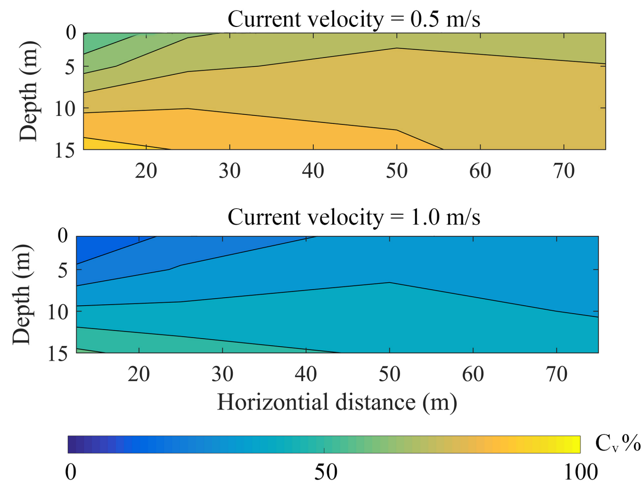

FIGURE 12. Fish cage volume remaining coefficients for the SPM with lower bridles in different conjunction point positions. (Depth: form the free surface to the conjunction point; Horizontal distance: from the wall of cage net to the conjunction point.)

Effect of conjunction point position

Adjusting the position of conjunction point for the SPM system with lower bridles will change the fish cage volume and tension force. In this sensitivity study, the buoy is assumed to have enough buoyancy force to keep it on the free surface. Sixteen cross-combinations with four different depths (2m, 5m, 10m and 15m) and four horizontal distances (12.5m, 25m, 50m and 75m) are employed in the mooring system for the case with lower bridles. The results are shown in Figure 12 where the volume remaining coefficient is represented by different colors. It indicates that the cultivation volume can become larger as the conjunction point is closer to the bottom ring. The cultivation volume can increase 28% (36%) when the current velocity =0.5m/s (1.0m/s), if the conjunction point is moved from the worst position to the optimal position. The worst position is near the floating collar, and that could be a reason why the lower bridles had no effect in Xu et al's research [7]. Figure 12 also indicates that the cultivation volume is not sensitive to the horizontal distance. In practice, there should be a safe distance between the floating collar and the buoy to avoid collisions; thus, the horizontal distance could not be too small. In addition, the tension forces on the anchor point are not changed significantly with the change of the conjunction point position.

CONCLUSIONS

A numerical study on a single-point mooring Norwegian fish cage with different deformation-suppression methods under the current and combined wave-current conditions has been carried out. The following conclusions are drawn from this study:

(a) In the harsh environmental conditions, the trawl door has the best performance in the cultivation volume maintaining, as it can reduce the volume loss by 56% compared to the original SPM fish cage when the current velocity is 1 m/s. However, it can also bring extra tension forces on the mooring system.
(b) The frontal frame is a solid method to hold the fish cage. However, the vertical distance between the upper and lower segment can be reduced due to the increased drag force on the net pen especially when the current velocity is higher than 0.5m/s. It can improve the cultivation volume by 44% compared to the original SPM fish cage when the current velocity is 1 m/s.
(c) Adding the lower bridles to the original SPM fish cage might cost less than any other methods. It can improve the cultivation volume by 34% compared to the original SPM fish cage when the current velocity is 1m/s.
(d) Wave effect is an important factor in the simulation as it can induce extra environmental loads and reduce the cultivation volume. The mean value of the cultivation volume is decreased with the decreasing wavelength, and the mean value of the tension force on the anchor point is increased with the decreasing wavelength.
(e) For the mooring system with lower bridles, moving the conjunction point close to the bottom ring can improve the effect of lower bridles with an unnoticeable increase in the tension force. The cultivation volume remaining coefficient can increase more than 28% when the current velocity is higher than 0.5 m/s, if the conjunction point is moved from the worst position to the optimal position.

ACKNOWLEDGMENT

The authors would like to thank Dr. Qingchang Xu from the Yellow Sea Fisheries Research Institute in Qingdao, China for kindly providing the parameters of trawl door.

REFERENCES

[1] Goudey, C. A., Loverich, G., Kite-Powell, H., and Costa-Pierce, B. A., 2001. "Mitigating the environmental effects of mariculture through single-point moorings (SPMs) and drifting cages". *ICES Journal of Marine Science,* ***58***(2), pp. 497–503.

[2] FAO, 2018. *The State of World Fisheries and Aquaculture 2018 - Meeting the sustainable development goals*. Licence: CC BY-NC-SA 3.0 IGO, Rome.

[3] Huang, C. C., Tang, H. J., and Pan, J. Y., 2009. "Numerical modeling of a single-point mooring cage with a frontal rigid frame". *IEEE Journal of Oceanic Engineering,* ***34***(2), pp. 113–122.

[4] Cheng, H., Huang, L., Ni, Y., Xu, Q., Zhao, F., Wang, X., and Liang, Z., 2018. "Numerical and experimental study of SPM fish cage: Comparison and validation". *International Conference on Offshore Mechanics and Arctic Engineering*(51272), pp. OMAE2018–78204.

[5] Lopez, J., Hurtado, F., Queirolo, D., Zamora, V., and Suazo, G., 2015. "Volume loss of an aquaculture net pen due to current speed and linear weight of sinker ring". *Latin American Journal of Aquatic Research,* ***43***(2), pp. 309–314.

[6] Huang, C. C., Tang, H. J., and Wang, B. S., 2010. "Numerical modeling for an in situ single-point-mooring cage system". *IEEE Journal of Oceanic Engineering,* ***35***(3), pp. 565–573.

[7] Xu, T. J., Dong, G. H., Li, Y. C., and Guo, W. J., 2014. "Numerical study of a self-submersible single-point mooring gravity cage in combined wave-current flow". *Applied Ocean Research,* ***48***, pp. 66–79.

[8] Xu, T.-j., Dong, G.-h., and Li, Y.-c., 2015. "Analysis of a self-submersible single-point mooring gravity cage in waves and current". In Twenty-fifth (2015) International Ocean and Polar Engineering, International Society of Offshore and Polar Engineers (ISOPE), pp. 1025–1031.

[9] Siddiqui, M. A., and Nagarajan, V., 2016. "Dynamics of a Single Point Mooring Marine Aquaculture Cage as a Simple Vibrating System". *INTERNATIONAL JOURNAL OF MARITIME TECHNOLOGY,* ***5***, pp. 13–25.

[10] Shainee, M., Leira, B. J., Ellingsen, H., and Fredheim, A., 2014. "Investigation of a self-submersible SPM cage system in random waves". *Aquacultural Engineering,* ***58***, pp. 35–44.

[11] Emmanuel, A., and Olivares, V., 2003. Design of a Cage Culture System for Farming in Mexico. Tech. rep., Instituto Tecnologico Del Mar En Mazatln.

[12] Hansen, T., Stefansson, S., Taranger, G., and Norberg, B., 2000. "Aquaculture in norway". In International Symposium on the Reproductive Physiology of Fish.

[13] Chang, Q., Lei, C., Yi, L., Qiang, J., Wang, L., Zhang, X., Lin, Z., Li, Y., Fang, F., Xin, X., and Cheng, H., 2018. "Parameter optimization of a double-de fl ector rectangular cambered otter board : Numerical simulation study". *Ocean Engineering,* ***162***(May), pp. 108–116.

[14] Reite, K.-j., Føre, M., Aarsæther, K. G., Jensen, J., Rundtop, P., Kyllingstad, L. T., Endresen, P. C., Kristiansen, D., Johansen, V., and Fredheim, A., 2014. "FHSIM TIME DOMAIN SIMULATION OF MARINE SYSTEMS". In Proceedings of the ASME 2014 33rd International Conference on Ocean, Offshore and Arctic Engineering, no. 1, pp. 1–10.

[15] Endresen, P. C., Birkevold, J., Føre, M., Fredheim, A., Kristiansen, D., and Lader, P., 2014. "Simulation and validation of a numerical model of a full aquaculture net cage system". In Proceedings of the ASME 2014 33rd International Conference on Ocean, Offshore and Arctic Engineering, no. 1, pp. 1–11.

[16] Endresen, P. C., Føre, M., Fredheim, A., Kristiansen, D., and Enerhaug, B., 2013. "NUMERICAL MODELING OF WAKE EFFECT ON AQUACULTURE NETS". In Proceedings of the ASME 2014 33rd International Conference on Ocean, Offshore and Arctic Engineering, pp. 1–10.

[17] Enerhaug, B., Føre, M., Endresen, P. C., Madsen, N., and Hansen, K., 2012. "Current loads on net panels with rhombic meshes". *Proceedings of the ASME 2012 31th International Conference on Ocean, Offshore and Arctic Engineering OMAE 2011*, pp. 1–12.

[18] Goldstein, S., 1965. *Modern Developments in Fluid Dynamics*. Dover Publications.

[19] Blevins, R. D., 1984. "Applied fluid dynamics handbook". *New York, Van Nostrand Reinhold Co., 1984, 568 p.*

[20] Fredriksson, D. W., Decew, J., Lader, P., Volent, Z., Jensen, and Willumsen, F. V., 2014. "A finite element modeling technique for an aquaculture net with laboratory measurement comparisons". *Ocean Engineering,* ***83***, pp. 99–110.

[21] Priour, D., 2013. *A Finite Element Method for Netting: Applications to Fish Cages and Fishing Gear*. Springer.

[22] Zhao, F., Kinoshita, T., Bao, W., Wan, R., Liang, Z., and Huang, L., 2011. "Hydrodynamics identities and wave-drift force of a porous body". *Applied Ocean Research,* ***33***(3), pp. 169–177.

[23] Huang, L., 2013. "Study on hydrodynamic characteristics of circular hdpe sea cage system with double floating tubes". PhD thesis, Ocean University of China.